

## Effect of nuclear mass on carrier-envelope-phase-controlled electron localization in dissociating molecules

Han Xu,<sup>1</sup> Tian-Yu Xu,<sup>2</sup> Feng He,<sup>2,\*</sup> D. Kielpinski,<sup>1,3</sup> R. T. Sang,<sup>1,3</sup> and I. V. Litvinyuk<sup>1,†</sup>

<sup>1</sup>Centre for Quantum Dynamics and Australian Attosecond Science Facility, Griffith University, Nathan, QLD 4111, Australia

<sup>2</sup>Key Laboratory for Laser Plasmas (Ministry of Education) and Department of Physics and Astronomy, SJTU, Shanghai 200240, People's Republic of China

<sup>3</sup>ARC Centre of Excellence for Coherent X-Ray Science, Griffith University, Nathan, QLD 4111, Australia

(Received 26 November 2013; published 15 April 2014)

We explore the effect of nuclear mass on the laser-driven electron localization process. We dissociate a mixed H<sub>2</sub> and D<sub>2</sub> target with intense, carrier-envelope-phase (CEP) stable 6 fs laser pulses and detect the products in a reaction microscope. We observe a very strong CEP-dependent asymmetry in proton and deuteron emission for low dissociation energy channels. This asymmetry is stronger for H<sub>2</sub> than for D<sub>2</sub>. We also observe a large CEP offset between the asymmetry spectra for H<sub>2</sub> and D<sub>2</sub>. Our theoretical simulations, based on a one-dimensional two-channel model, agree very well with the asymmetry spectra, but fail to account properly for the phase difference between the two isotopes.

DOI: [10.1103/PhysRevA.89.041403](https://doi.org/10.1103/PhysRevA.89.041403)

PACS number(s): 33.80.Wz, 42.50.Hz

Coherent control of molecular fragmentation with few-cycle laser pulses of well-defined carrier-envelope phase (CEP) has become an active research topic in ultrafast science due to its potential application for control of chemical reactions. In particular, molecular hydrogen (H<sub>2</sub>) and its heavy isotope deuterium (D<sub>2</sub>) have attracted a lot of attention [1–7], since these simple molecules can help us understand how more complicated larger molecules interact with strong laser fields. Even for simple molecules, complete *ab initio* treatment is still a daunting task and approximate models continue to be commonly used. It is therefore important to explore the validity and limitations of those approximate models by comparing their predictions with experimental observations. Any such quantitative comparison would usually require a precise knowledge of laser parameters, and must also take into account temporal and spatial variations of those parameters over the interaction region. Studying the isotope dependence allows one to keep all the parameters constant while focusing on a singular effect of nuclear mass. Here we report such experimental comparative study of CEP-dependent dissociation in H<sub>2</sub> and D<sub>2</sub>.

The CEP control of dissociative ionization of D<sub>2</sub> with 5 fs  $1 \times 10^{14}$  W/cm<sup>2</sup> laser pulses was first demonstrated by Kling *et al.* [1]. That study reported a significant (~20%) CEP-dependent asymmetry for a channel with high kinetic energy release (KER). Their result was attributed to the recollision excitation from the bound ground  $1s\sigma_g$  (gerade) state directly to the repulsive excited  $2p\sigma_u$  (ungerade) state of D<sub>2</sub><sup>+</sup>, shortly after the first ionization of D<sub>2</sub>. However, no significant asymmetry was observed by Kling and co-workers in the dominant low-KER region, which corresponds to radiative excitation and deexcitation channels. In another experiment with H<sub>2</sub>, Kremer *et al.* [2] reported a pronounced asymmetry modulation of ~15% for low-KER channels with significantly higher laser

intensity ( $4 \times 10^{14}$  W/cm<sup>2</sup>). In our own experiments on H<sub>2</sub> with even more intense pulses ( $6 \times 10^{14}$  W/cm<sup>2</sup>), we observed a very high CEP-dependent asymmetry of 40%, as well as modulation of up to 5% in dissociation yield [3]. More recently, studies of CEP-dependent dissociation using an H<sub>2</sub><sup>+</sup> ion beam have also been reported [8,9]. These experiments used 4.5 [8] and 5 fs [9] pulses of  $4 \times 10^{14}$  W/cm<sup>2</sup> peak intensity and also measured significant asymmetry, up to 30% for [8], in the low-KER channels. None of those experimental studies makes a comparison between the two isotopes of hydrogen. H<sub>2</sub><sup>+</sup> and D<sub>2</sub><sup>+</sup> remain the only targets for which full dimensionality *ab initio* theoretical modeling of laser-induced dissociation is currently feasible; however, these are only applicable within the Born-Oppenheimer approximation [10] and for sufficiently low intensities avoiding ionization [9].

In general, low-KER ions are produced via radiative excitation and deexcitation by absorbing and emitting a certain number of photons from the driving laser field at large internuclear separations. Figure 1 shows the evolution of the molecular potential and the major dissociation channels, which were identified some time ago using multicycle laser pulses. Low-KER dissociation occurs through bond softening (BS; net one-photon process [11]) and above-threshold dissociation (ATD; net two-photon process [12]). Some later experimental [13] and theoretical [14] work indicated that a net three-photon process (TPD) might also be relevant to hydrogen dissociation. According to the general theory of CEP effects [15], CEP-dependent asymmetries can be interpreted in terms of interfering quantum pathways with different (by odd number, mostly  $\Delta n = 1$ ) numbers of absorbed photons. The relevant dissociation pathways are shown in Fig. 1(a). To observe the interference, the KER spectra for the interfering channels must overlap, so that broadband (few-cycle) pulses are required for CEP-controlled asymmetry. Optimal asymmetry modulations will be achieved when the two interfering pathways have similar transition amplitudes. That condition can only be satisfied at intensities of a few  $\times 10^{14}$  W/cm<sup>2</sup>, an order of magnitude higher than in the original experiment by Kling and co-workers [1].

\*fhe@sjtu.edu.cn

†i.litvinyuk@griffith.edu.au

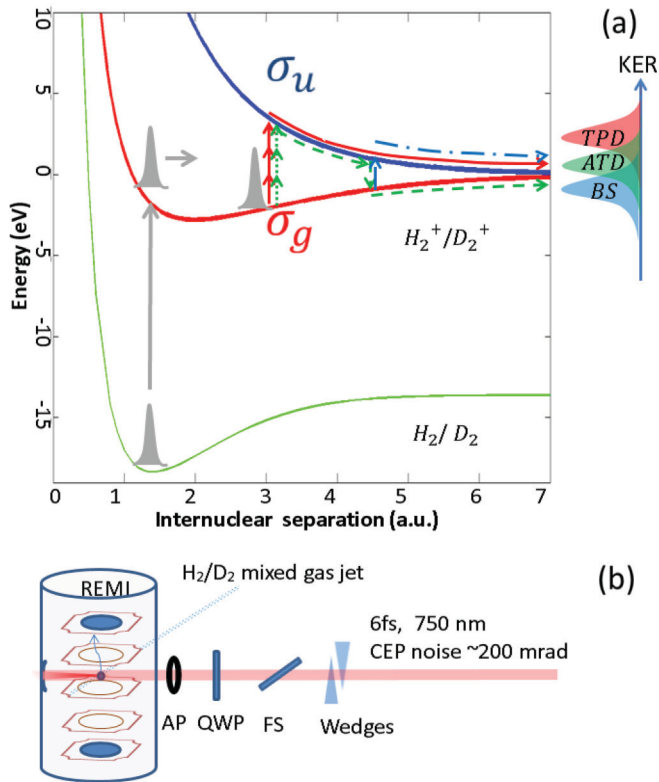


FIG. 1. (Color online) (a) The potential energy curves and three relevant dissociation pathways for  $\text{H}_2^+$  and  $\text{D}_2^+$  (see text for discussion). The arrows represent transitions corresponding to the central wavelength of the driving few-cycle laser pulse. Its broad spectral bandwidth leads to broad and overlapping  $\text{H}^+$  and  $\text{D}^+$  KER spectra allowing interference between the dissociation pathways. (b) Schematic diagram of the experiment (REMI: reaction microscope; AP: aperture; QWP: quarter-wave plate; FS: fused silica plate).

Nuclear mass also plays an important role in the observation of CEP-dependent asymmetries. Since we start with a neutral molecule in its ground state, the ionization creates a dynamic nuclear wave packet propagating on the ground-state potential energy surface of molecular ion. That molecular ion will resonantly absorb (and sometimes also emit) photons from the field later during the laser pulse, as the nuclear wave packet continues its propagation towards dissociation along various pathways. The timing and probability of those resonant radiative transitions will sensitively depend on wave-packet velocity, which in turn depends on nuclear mass. For example, the nuclei in  $\text{H}_2^+$  move faster and will reach the coupling region sooner than the heavier  $\text{D}_2^+$  nuclei, so they experience higher intensities in the falling edge of the laser pulse. It is therefore expected that CEP control of electron localization will also be very sensitive to nuclear mass.

A pioneering theoretical work [16] has discussed such mass effect in dissociation of isotopes of hydrogen ions, while no supporting experimental evidence has been reported so far. The dissociation of various isotopes of a hydrogen molecule has been studied experimentally in previous works [1,2,17], but a direct comparison of those experiments is not possible due to the influence of different laser parameters (intensity, pulse duration, CEP, and focusing geometry). Here, we present

an experiment performed with a  $\text{H}_2$  and  $\text{D}_2$  mixed-gas target interacting with a CEP-stabilized few-cycle laser pulse. By properly selecting the laser intensity, a strong CEP-dependent asymmetry for both  $\text{H}_2$  and  $\text{D}_2$  is observed. In a mixed-gas jet, the  $\text{H}_2$  and  $\text{D}_2$  molecules will experience exactly the same laser parameters. Hence, the measured CEP dependence for  $\text{H}_2$  and  $\text{D}_2$  is suitable for quantitative study of the role of nuclear mass in the CEP-controlled molecular fragmentation which is free of systematic errors. We focus our attention on low-KER ( $<4$  eV) fragments: At the intensities used in our experiment, more energetic fragments are dominated by double ionization, which obviously cannot display any asymmetry.

Our experimental apparatus is shown in Fig. 1(b), and its detailed description can be found in our previous paper [3]. The pulse duration of the few-cycle laser is measured to be  $\sim 6$  fs (FWHM of intensity profile). The CEP of the pulse is stabilized by using a feedback loop based on an  $f$ - $2f$  interferometer (Menlo Systems), and is manipulated by rotating a piece of fused silica plate around Brewster's angle. The laser beam is focused with a 75 mm focal length spherical mirror onto a supersonic mixed-gas jet, which contains 50%  $\text{H}_2$  and 50%  $\text{D}_2$ . A very small amount ( $<1\%$ ) of HD molecules is also observed in the experiment, but its influence on the measurement could be neglected. The width of the mixed-gas jet is localized along the laser propagation direction to  $<100$   $\mu\text{m}$  by an adjustable slit, which is much smaller than the Rayleigh length ( $\sim 700$   $\mu\text{m}$ ) of the laser beam. This helps us minimize the influence of the Gouy phase effect and focal volume averaging effect, yielding higher asymmetry modulation. Before entering the REMI chamber, the laser beam is truncated by an adjustable iris to tune the laser intensity in the interaction region. A quarter-wave plate is employed to switch the polarization of the laser between linear and circular without affecting the pulse duration. Circularly polarized pulses are used to ionize a neon jet, and the laser peak intensity is calibrated *in situ* by measuring the momentum distribution of  $\text{Ne}^+$  ions [18,19]. The electric field of the linearly polarized pulse is parallel to the time-of-flight axis of REMI and perpendicular to both laser beam and gas jet propagation directions. The  $\text{H}^+$  and  $\text{D}^+$  fragments are steered by a static electric field, which is high enough to avoid overlapping of the time-of-flight spectra of  $\text{H}^+$  and  $\text{D}^+$ , towards a time- and position-sensitive detector, where their three-dimensional momentum vectors are determined.

The experimental KER spectra as well as KER- and CEP-dependent asymmetry are shown in Figs. 2(a), 2(b), 2(e), and 2(f). As the strongest coupling occurs for molecules parallel to the laser polarization,  $\text{H}^+$  and  $\text{D}^+$  emitted into a small angle ( $\theta$ ) around the laser polarization are selected for analysis. For those ions emitted towards the detector (up),  $\theta > 30^\circ$  is selected, while for ions emitted away from the detector (down),  $\theta > 150^\circ$  is selected. The KER- and CEP-dependent asymmetry parameter is defined as

$$\alpha(\text{KER}, \varphi_{\text{CEP}}) = \frac{N_{\text{up}}(\text{KER}, \varphi_{\text{CEP}}) - N_{\text{down}}(\text{KER}, \varphi_{\text{CEP}})}{\overline{N_{\text{tot}}}(\text{KER})}, \quad (1)$$

where  $N_{\text{up}}$  and  $N_{\text{down}}$  are the ion yield in the up and down directions, respectively, and  $\overline{N_{\text{tot}}}$  is the CEP averaged total ion yield in both directions. As predicted in Ref. [16],  $N_{\text{up}} - N_{\text{down}}$  can be expressed as a sinusoidal function of CEP with a

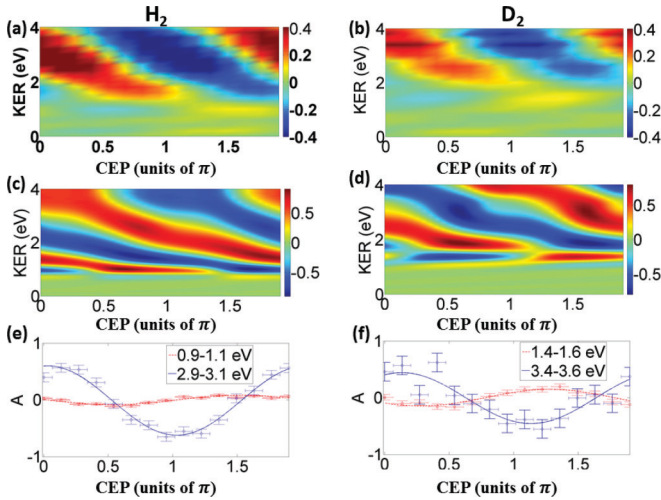


FIG. 2. (Color online) Experimental asymmetry as a function of relative CEP and KER for  $H_2$  (a) and  $D_2$  (b) with 6 fs pulses of peak intensity  $8(\pm 2) \times 10^{14}$  W/cm $^2$ . (c) and (d) show the results of our two-state model calculations for  $H_2$  and  $D_2$ , respectively, with the same laser parameters as used in the experiment. (e) and (f) demonstrate the measured (markers) CEP-dependent asymmetry and their sine curve fittings (lines) of  $H_2$  (e) and  $D_2$  (f) for selected KER regions specified in the insets.

phase offset, when only interference of neighboring ( $\Delta n = 1$ ) photon channels is important. However, the bandwidth of 6 fs pulse is broad enough to support interference between  $n$  and  $n+2$  photon channels, which will lead to a  $\pi$ -periodic modulation of  $N_{\text{tot}}$  as a function of CEP. We observed such a modulation at the 5% level previously [3]. Consequently, the asymmetry parameter defined in a traditional way as  $(N_{\text{up}} - N_{\text{down}})/(N_{\text{up}} + N_{\text{down}})$  will not be a simple sine function of CEP. To correct for this, we use CEP averaged  $\overline{N_{\text{tot}}}(\text{KER})$  instead of  $N_{\text{tot}}$  so that the asymmetry parameter can be described by

$$\alpha(\text{KER}, \varphi_{\text{CEP}}) = A(\text{KER})\sin[\varphi_{\text{CEP}} + B(\text{KER})], \quad (2)$$

where  $A$  and  $B$  are the KER-resolved amplitude and phase shift parameter of the asymmetry modulation, respectively. The measured CEP-dependent asymmetry for  $H_2$  and  $D_2$  is then fitted by Eq. (2) to retrieve the  $A$  and  $B$  parameters, which are presented in Figs. 3(b) and 3(c).

We compare our experimental results with theoretical calculations based on a one-dimensional two-channel approximation to the time-dependent Schrödinger equation (TDSE). Figure 2 shows the results of these calculations. We model the first ionization step, which creates the molecular ion, by projecting the neutral ground-state nuclear wave packet onto the  $1s\sigma_g$  state of the molecular ion (Franck-Condon approximation). In the Born-Oppenheimer approximation, the wave function of the molecular ion can be expressed as  $\varphi(R, \vec{x}, t) \approx \chi_g(R, t)\varphi_g(R, \vec{x}) + \chi_u(R, t)\varphi_u(R, \vec{x})$ , where  $R$  is the internuclear separation,  $x$  denotes the electronic coordinate,  $\varphi_g(R, \vec{x})$  and  $\varphi_u(R, \vec{x})$  are the two lowest electronic states with opposite parities,  $1s\sigma_g$  and  $2p\sigma_u$ , with potential energy curves for these states given by  $V_g(R)$  and  $V_u(R)$ . The

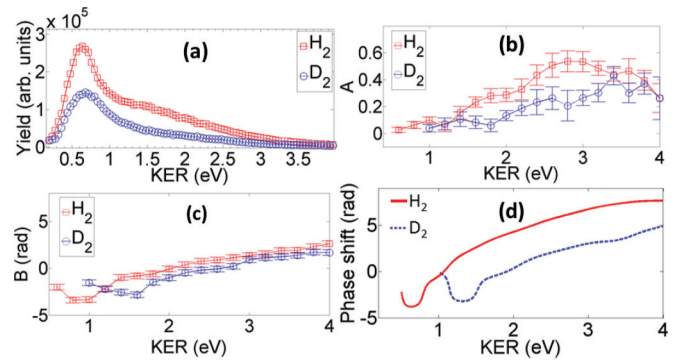


FIG. 3. (Color online) (a) Experimental KER spectra integrated over all CEP values for  $H_2$  and  $D_2$ . The KER-dependent  $A$  parameter (b) and  $B$  parameter [(c),(d)] retrieved by fitting the experimental (c) and simulated (d) CEP-dependent asymmetry with function (2) for both  $H_2$  and  $D_2$  (see text for details).

corresponding nuclear wave functions are denoted  $\chi_g(R, t)$  and  $\chi_u(R, t)$ .

We now solve the following two-channel TDSE equation [2,4], with initial wave packets created at each local maximum of the few-cycle pulse, and their relative probabilities are weighted according to the Ammosov-Delone-Krainov [20] ionization rate:

$$i \frac{\partial}{\partial t} \begin{pmatrix} \chi_g(R, t) \\ \chi_u(R, t) \end{pmatrix} = \begin{pmatrix} T_R + V_g(R) & V_{gu}(R, t) \\ V_{gu}(R, t) & T_R + V_u(R) \end{pmatrix} \begin{pmatrix} \chi_g(R, t) \\ \chi_u(R, t) \end{pmatrix}, \quad (3)$$

where  $T_R = -\frac{1}{2\mu} \frac{\partial^2}{\partial R^2}$ ,  $\mu$  is the reduced mass, and  $V_{gu}(R, t)$  is the dipole coupling. In our simulation, the spatial and temporal steps are  $\delta R = 0.04$  a.u. and  $\delta t = 1$  a.u. The spatial grid covers the range  $R = 0-500$  a.u.. In this model, we assume that the molecular axis is parallel to the laser, and ignore molecular rotations. Focal volume averaging and Gouy phase variation are also ignored in the calculation. Since the thickness of the molecular beam in the experiment is much smaller than the Rayleigh range of the laser focus, those effects should not significantly affect the results.

As seen from Fig. 2, the asymmetry results for  $H_2$  and  $D_2$  are qualitatively similar, with two distinct energy regions characterized by different modulation depths with opposite tilting of the stripes in the asymmetry spectra. For  $H_2$ , the two energy regions are  $\text{KER} < 1.3$  eV and  $\text{KER} > 1.3$  eV, which are assigned as corresponding to BS-ATD interference and ATD-TPD interference [3], respectively. For  $D_2$ , the two energy regions are  $\text{KER} < 1.8$  eV and  $\text{KER} > 1.8$  eV, with the boundary shifted by 0.5 eV to higher energy. That energy shift is reproduced by the model calculation of this work. We note that similar energy shifts in hydrogen molecular ion and its heavier isotopes have also been predicted theoretically in [16]. In Figs. 2(e) and 2(f), a KER window is selected for each energy region, within which the asymmetry curves are calculated and presented. To address the observed 0.5 eV shift, the KER windows for  $D_2$  [see Fig. 2(f)] are shifted towards higher energy by 0.5 eV compared to those for  $H_2$  [see Fig. 2(e)]. The asymmetry modulation depth for  $H_2$

in the ATD-TPD region could be as high as 50%, while for  $D_2$  a somewhat lower 40% modulation is observed. The calculated asymmetry [Figs. 2(c) and 2(d)] agrees very well with experimental results for both molecules.

A comparison of the experimental data for  $H^+$  and  $D^+$  reveals three main differences between the two isotopes: (i) The total dissociation yield is much higher (almost twice for BS and even more for ATD and TPD) for the light isotope [Fig. 3(a)]. That is likely due to the fact that in  $H_2^+$  the nuclear wave packet reaches the strong-coupling region faster than in  $D_2^+$  and experiences higher intensities and higher radiative transition rates. (ii) The asymmetry modulation amplitude is somewhat larger for the light isotope, particularly for  $KER > 2$  eV corresponding to ATD-TPD interference [Fig. 3(b)]. That is due to the higher relative population of the TPD pathway in  $H_2^+$ , which also can be explained by its faster expansion into the radiative coupling region. (iii) The CEP-dependent asymmetry does not maximize at the same CEP for the two isotopes—there is a substantial phase shift in both experimental and theoretical asymmetry plots [Figs. 3(c) and 3(d)]. This phase shift is not unexpected—the phase will accumulate at different rates as different isotopes propagate along different pathways. The phase difference between the two interfering pathways will determine the relative phase of the resulting CEP dependence. KER dependence of the phase (manifested as a tilt in the two-dimensional asymmetry plots) for the same two-channel interference has similar origin. It is noteworthy that the theory fails to predict the experimentally observed phase shift. The phase shift of  $\sim 1$  rad is measured for KER between 2 and 4 eV [Fig. 3(c)], while the theory predicts a much larger 3 rad phase difference between  $H_2$  and  $D_2$  [Fig. 3(d)]. Obviously, our simple one-dimensional model fails to properly account for the phase. The discrepancy could be due to neglect of rotations (much different for the two isotopes) and non-Born-Oppenheimer terms (more important for

$H_2^+$ ) or due to the omitted interference of the nuclear wave packet generated in different optical cycles. Regardless of the reasons, a note of caution is due here. By looking at the good agreement between theory and experiment for each of the two isotopes taken separately (Fig. 2), one might be tempted to use that comparison for an absolute CEP calibration. However, a side-by-side comparison of the two isotopes immediately reveals that the theoretical model does not reproduce the phase correctly and therefore cannot be used for such absolute CEP measurement. More generally, one has to be particularly careful when trying to extract absolute CEP information from *ad hoc* simplified models.

To conclude, we compare the CEP dependence of the dissociation of  $H_2$  and its heavy isotope  $D_2$  by intense CEP-stabilized few-cycle laser field under identical experimental conditions. We report very strong CEP-dependent asymmetry for either isotope—50% for  $H_2$  and 40% for  $D_2$ . Quantitative comparison of the two isotopes reveals significant mass effects, which can be generally explained by faster motion of lighter nuclei in  $H_2$ . While the overall agreement between the experiment and theoretical predictions is very good, our one-dimensional two-channel Born-Oppenheimer model fails to reproduce the phase difference between the two isotopes. A more realistic model will be required to account for that measurement.

This work was supported by an Australian Research Council (ARC) Discovery Project (DP110101894) and by the ARC Centre for Coherent X-Ray Science (Grant No. CE0561787). H.X. was supported by an ARC Discovery Early Career Researcher Award (DE130101628). F.H. acknowledges the financial support from NSFC (Grants No. 11104180, No. 11175120, No. 11121504, and No. 11322438) and NSF of Shanghai (Grant No. 11ZR1417100). D.K. was supported by an ARC Future Fellowship (FT110100513).

- 
- [1] M. F. Kling *et al.*, *Science* **312**, 246 (2006).  
 [2] M. Kremer *et al.*, *Phys. Rev. Lett.* **103**, 213003 (2009).  
 [3] H. Xu, J.-P. Maclean, D. E. Laban, W. C. Wallace, D. Kiełpinski, R. T. Sang, and I. V. Litvinyuk, *New J. Phys.* **15**, 023034 (2013).  
 [4] D. Ray *et al.*, *Phys. Rev. Lett.* **103**, 223201 (2009).  
 [5] G. Sansone *et al.*, *Nature (London)* **465**, 763 (2010).  
 [6] K. P. Singh *et al.*, *Phys. Rev. Lett.* **104**, 023001 (2010).  
 [7] I. Znakovskaya *et al.*, *Phys. Rev. Lett.* **108**, 063002 (2012).  
 [8] T. Rathje, A. M. Sayler, S. Zeng, P. Wustelt, H. Figger, B. D. Esry, and G. G. Paulus, *Phys. Rev. Lett.* **111**, 093002 (2013).  
 [9] N. G. Kling *et al.*, *Phys. Rev. Lett.* **111**, 163004 (2013).  
 [10] F. Anis and B. D. Esry, *Phys. Rev. A* **77**, 033416 (2008).  
 [11] P. H. Bucksbaum, A. Zavriyev, H. G. Muller, and D. W. Schumacher, *Phys. Rev. Lett.* **64**, 1883 (1990).  
 [12] A. Giusti-Suzor, X. He, O. Atabek, and F. H. Mies, *Phys. Rev. Lett.* **64**, 515 (1990).  
 [13] S. Chelkowski, A. D. Bandrauk, A. Staudte, and P. B. Corkum, *Phys. Rev. A* **76**, 013405 (2007).  
 [14] I. V. Litvinyuk, A. S. Alnaser, D. Comtois, D. Ray, A. T. Hasan, J.-C. Kieffer, and D. M. Villeneuve, *New J. Phys.* **10**, 083011 (2008).  
 [15] V. Roudnev and B. D. Esry, *Phys. Rev. Lett.* **99**, 220406 (2007).  
 [16] J. J. Hua and B. D. Esry, *J. Phys. B: At., Mol. Opt. Phys.* **42**, 085601 (2009).  
 [17] M. F. Kling, Ch. Siedschlag, I. Znakovskaya, A. J. Verhoef, S. Zherebtsov, F. Krausz, M. Lezius, and M. J. J. Vrakking, *Mol. Phys.* **106**, 455 (2008).  
 [18] A. S. Alnaser, X. M. Tong, T. Osipov, S. Voss, C. M. Maharjan, B. Shan, Z. Chang, and C. L. Cocke, *Phys. Rev. A* **70**, 023413 (2004).  
 [19] C. Smeenk, J. Z. Salvail, L. Arissian, P. B. Corkum, C. T. Hebeisen, and A. Staudte, *Opt. Express* **19**, 9336 (2011).  
 [20] M. V. Ammosov, N. B. Delone, and V. P. Kraїnov, *Zh. Eksp. Teor. Fiz.* **91**, 2008 (1986) M. V. Ammosov, N. B. Delone, and V. P. Krainov, [*Sov. Phys. JETP* **64**, 1191 (1986)].